THE ANNALS OF "DUNĂREA DE JOS" UNIVERSITY OF GALAŢI
FASCICLE V, TECHNOLOGIES IN MACHINE BUILDING,
ISSN 1221- 4566, 2017

# THE GEOMETRIC ROUGHNESS WHEN MACHINING INVOLUTE GEAR TOOTH WITH FEED MOTION OF VARIABLE SPEED

Mihail Bordeanu, Gabriel Frumuşanu, Nicolae Oancea

"Dunărea de Jos" University of Galaţi, Romania, Manufacturing Engineering Department
gabriel.frumusanu@ugal.ro

## ABSTRACT

*The toothing process performed by enwrapping method presents high non-uniformities due to variation of removed chip area between successive cuts. A solution to this problem, based on varying the feed speed during the rolling motion has already been suggested and proved to be feasible. However, the feed motion practiced with variable speed impacts the geometric roughness of tooth flank generated surface. This paper investigates the degree to which feed speed variation after a given law affects the roughness of such a surface, by assessing the height of irregularities resulted between the successive trails left by tool teeth. An analytical solution and a graphical solution (the last one developed in CATIA graphical environment), addressing the case of using a mono-tooth rack-tool, are both presented and applied for an actual gear.*

**KEYWORDS:** involute gear, geometric roughness, variable feed speed, CATIA

## 1. INTRODUCTION

### *1.1. The geometric roughness*

The machined surfaces, no matter the cutting method, are affected by errors with negative effect onto the contact position with possible conjugated surfaces. If about gear pairs, then transmitted motion is affected from kinematical point of view and the dynamics of gear system may also suffer.

The technology of surfaces generation involves irregularities of machined surface due, among others, to theoretical errors of generating the surface caused by the intermittent contact of cutting tool teeth with the machined surface. The analytical models for surfaces generation can input surfaces generating errors, which may be defined as "geometric" errors. Added to this, the effects of chip removal process, of removed material behaviour and of cutting liquids increase the machined surface roughness.

As the machined surface quality is a topic of high interest, many researches have addressed the geometrical roughness subject, from different points of view, using diverse techniques. For example, [1] examines the influence of the milling strategy selection on the surface roughness of an Al7075-T6 alloy, a mathematical model of the surface roughness being established, considering both the down and up milling. Another work, [2], focuses on Ti–6Al–4V ELI titanium alloy machining by means of plain peripheral down milling process and subsequent modeling of this process, in order to predict surface quality of the workpiece and identify optimal cutting parameters, that lead to minimum surface roughness. Paper [3] focuses on Ti–6Al–4V ELI titanium alloy machining by means of plain peripheral down milling process and subsequent modeling of this process, the model being based on a geometrical analysis of the recreation of the tool trail left on the machined surface. Based on an improved Z-map model, a 3D simulation model of surface topography, to simulate the surface finish profile generated after a helical milling operation using a cylindrical end mill, is presented in [4]. The surfaces generated by turning has also been modeled in the mentioned purpose, e.g. [5] presents the concept of calculating a "pseudo-roughness" value based only on tool tip locations, and compare this value was compared to that determined by full predictive modeling of the tool geometry.

### *1.2. Problem definition*

In gear teeth machining, the analysis of tooth space generating process have been already realized and presented, e.g. in [6]. By addressing the case of a mono-tooth rack shaped cutter it proves that, during the toothing process, the area of the chip detached by tool cutting edge shows high variation when determined for successive rolling positions considered for the couple of centrodes attached to both tool and workpiece. This lack of uniformity leads to occurrence of highly variable cutting specific stress, depending on the tool position relative to the workpiece, with direct impact on the magnitude of main cutting force. In [7], we have already presented a solution to uniform the tooth space generating process by adopting a non-uniform process of rolling between the conjugated centrodes attached to both tool and workpiece, achieved by discrete variation of workpiece circular feed, after an appropriate law, as presented in Fig. 1.

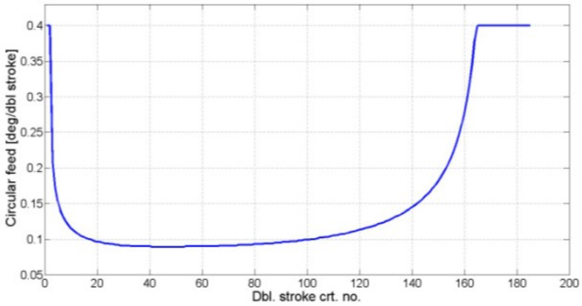


Fig. 1: Circular feed variation law [7]

The variation of feed motion speed obviously impacts the roughness of generated tooth flank. If the feed motion speed passes over the value that is used when machining with constant feed, then the geometric roughness might become too high. This paper investigates the degree to which feed speed variation after a given law affects the roughness of such a surface, by assessing the height of irregularities resulted between the successive trails left by tool teeth. An analytical solution and a graphical solution (the last one developed in CATIA graphical environment), addressing the case of using a mono-tooth rack-tool, are both presented and applied for an actual gear. The next section presents the analytical model of toothing process. The third section presents the analytical and the graphical methods for measuring the geometric roughness. The fourth section deals with numerical application of both methods, while the last one is for conclusion.

## 2. ANALYTICAL MODELLING OF THE TOOTHING PROCESS

In Fig. 2, it is depicted the principle of generating the gear tooth with a mono-tooth rack tool. Beside the specific kinematics, one may notice the two centrodes, $C_1$ (gear centrode, circle of $R_r$ radius) and $C_2$ (tool centrode, straight line tangent to $C_1$), and the following reference systems, needed in order to find the equations of tool / gear relative motion:

- *xyz*, meaning a global, fix system, having the origin into gear symmetry centre, *O*
- *XYZ* – relative system, initially overlapped to *xyz* and having a rotation motion of $\varphi$ angular parameter, together with gear around *O* point
- $\xi\eta\zeta$ – relative system, having the origin in centrodes tangency point, $O_1$, and translating together with tool along $C_2$, of $\lambda$ parameter.

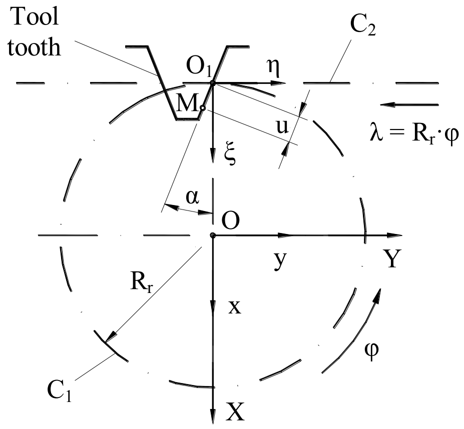


Fig. 2. Generating process kinematics & reference systems

The rolling condition can be expressed as:

$$\lambda = R_r \cdot \varphi . \tag{1}$$

The equations of gear and tool absolute motions are, respectively:

$$x = \omega_3^T(\varphi) \cdot X , \tag{2}$$

and

$$x = \xi + a \text{, with } a = \begin{pmatrix} -R_r \\ -R_r \cdot \varphi \end{pmatrix} . \tag{3}$$

Because we deal with plane motions (the speed vector of a given point remains permanently in a plane normal to *z* axis), kinematics equations will be also written in plane. The equation of relative motion between gear and tool results from (1) and (2), after eliminating *x*:

$$X = \omega_3(\varphi)[\xi + a], \tag{4}$$

where $\omega_3(\varphi)$ means the coordinates transform matrix for rotation around *z* axis. If in (4) the vector $\xi$ comprises the coordinates of current point from rack tooth flank, in $\xi\eta$ system (Fig.2):

$$\begin{vmatrix} \xi = u \cdot \cos\alpha ; \\ \eta = -u \cdot \sin\alpha , \end{vmatrix} \tag{5}$$

with *u* meaning a variable parameter, then, after developing calculus, from (4) we get:

$$\begin{vmatrix} X = (u \cdot \cos\alpha - R_r)\cos\varphi - (u \cdot \sin\alpha + R_r \cdot \varphi)\sin\varphi ; \\ Y = -(u \cdot \cos\alpha - R_r)\sin\varphi - (u \cdot \sin\alpha + R_r \cdot \varphi)\cos\varphi . \end{vmatrix} \tag{6}$$

In what concerns the values of *u* from (5), they are comprised between

$$u_{\min} = -\frac{1.2 \cdot m}{\cos\alpha} \text{ and } u_{\max} = \frac{1.2 \cdot m}{\cos\alpha}. \quad (7)$$

The equations (6) represent a straight lines family, meaning the successive positions of rack tooth flank relative to gear. The envelop of (6) family is the involute profile of generated tooth, and it can be found by associating to (6) the enveloping condition, which can be expressed, in its turn, by using the Minimum distance method [8]. According to this, the enveloping condition results by imposing to the distance $d$ between the current point from rack tooth flank ($M$, see Fig. 2) and gearing pole $P$ the condition of minimum:

$$d = \sqrt{(X_M - X_P)^2 + (Y_M - Y_P)^2} = \min. \quad (8)$$

The coordinates of $M$ are given by (6), while $P$ coordinates, expressed into $XY$ system, are:

$$\left| \begin{array}{l} X_P = -R_r \cdot \cos\varphi; \\ Y_P = R_r \cdot \sin\varphi. \end{array} \right. \quad (9)$$

The condition of minimum requires annulling the derivative of $d$ against $u$ variable:

$$[X_M(u) + R_r \cdot \cos\varphi]\dot{X}_{Mu} + [Y_M(u) - R_r \cdot \sin\varphi]\dot{Y}_{Mu} = 0 \quad (10)$$

After substitutions and calculus, the final form of enveloping condition is:

$$u = -R_r \cdot \varphi \cdot \sin\alpha. \quad (11)$$

By replacing (11) in (6) we obtain the equations of generated tooth flank $I$, referred to $XY$ system, as:

$$I \left| \begin{array}{l} X = -R_r \cdot \varphi \cdot \sin\alpha \cdot \cos(\alpha + \varphi) - R_r \cdot \cos\varphi - \\ \quad - R_r \cdot \varphi \cdot \sin\varphi; \\ Y = R_r \cdot \varphi \cdot \sin\alpha \cdot \sin(\alpha + \varphi) + R_r \cdot \sin\varphi - \\ \quad - R_r \cdot \varphi \cdot \cos\varphi. \end{array} \right. \quad (12)$$

## 3. THE GEOMETRIC ROUGHNESS

### *3.1. Analytical approach*

The equations (6) mean, as already mentioned, the family of rack tooth flank positions referred to gear system $XY$. Hereby, if in (6) one gives to $\varphi$ the values corresponding to two successive cuts of tool tooth, $\varphi_i$ and $\varphi_{i+1}$, then the resulted equations will represent two straight lines, $\Delta_i$ and $\Delta_{i+1}$, which intersect in $N_i$ point (Fig. 3). The distance between $N_i$ and the theoretical generated profile $I$ (12) represents the local value of geometric roughness.

We further suggest an analytical algorithm to assess the geometric roughness in the addressed case.

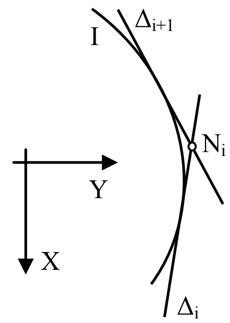


Fig. 3. Successive positions of the cutting edge

The equations of $\Delta_i$ and $\Delta_{i+1}$ are:

$$\Delta_i \left| \begin{array}{l} X = u \cdot \cos(\alpha + \varphi_i) - R_r \cdot \cos\varphi_i - R_r \cdot \varphi_i \cdot \sin\varphi_i; \\ Y = -u \cdot \sin(\alpha + \varphi_i) + R_r \cdot \sin\varphi_i - R_r \cdot \varphi_i \cdot \cos\varphi_i, \end{array} \right. \quad (13)$$

$$\Delta_{i+1} \left| \begin{array}{l} X = u^* \cdot \cos(\alpha + \varphi_{i+1}) - R_r \cdot \cos\varphi_{i+1} - \\ \quad - R_r \cdot \varphi_{i+1} \cdot \sin\varphi_{i+1}; \\ Y = -u^* \cdot \sin(\alpha + \varphi_{i+1}) + R_r \cdot \sin\varphi_{i+1} - \\ \quad - R_r \cdot \varphi_{i+1} \cdot \cos\varphi_{i+1}. \end{array} \right. \quad (14)$$

The coordinates of intersection point $N_i$ can be obtained by equalizing $X$ and $Y$ from (13) with $X$ and $Y$ from (14), respectively. The solution of this system will consist in a couple of values for $u$ and $u^*$ variables, which replaced in (13) and (14) will give as well $N_i$ coordinates, ($X_{Ni}$, $Y_{Ni}$).

The directional coefficients of $N_\Sigma$ normal to $I$ curve, written in the current point, result from:

$$\overrightarrow{N_\Sigma} = \begin{vmatrix} \vec{i} & \vec{j} \\ \dot{X}_\varphi & \dot{Y}_\varphi \end{vmatrix}, \quad (15)$$

hence normal equations are:

$$\overrightarrow{N_\Sigma} \left| \begin{array}{l} X = X(\varphi) + \lambda \cdot \dot{Y}_\varphi; \\ Y = Y(\varphi) - \lambda \cdot \dot{X}_\varphi. \end{array} \right. \quad (16)$$

In relations (15) and (16), the expressions of $X$ and $Y$ are the ones from (12), while $\lambda$ is a variable parameter.

By imposing the condition that the normal to profile $I$ should pass through point $N_i$, we obtain the following equations system:

$$\begin{cases} X(\varphi) + \lambda \cdot \dot{Y}_\varphi = X_{N_i} \\ Y(\varphi) - \lambda \cdot \dot{X}_\varphi = Y_{N_i} \end{cases}. \quad (17)$$

The solution of the system from above will be a couple of values ($\varphi_i$, $\lambda_i$). We can finally notice, in the end, that $\lambda_i$ value means, in fact, the distance between $N_i$ point and $I$ curve, hence the geometric roughness corresponding to the space from $i^{th}$ and $(i + 1)^{th}$ cuts of the rack tool tooth.

### *3.2. Graphical approach*

The geometrical roughness of gear tooth flank generated with a mono-tooth rack tool can also be found by using the facilities of CATIA graphical environment. In this purpose, we suggest the following algorithm:

- solid models of both workpiece and tool tooth are built by using *Sketch* module of CATIA. First, the workpiece is sketched and geometrical/dimensional constrains are applied to it. Workpiece model is a cylindrical disc having the exterior diameter equal to head diameter of the gear to be generated. The condition of tangency between rack shaped cutter rolling line and workpiece rolling circle is also imposed (Fig. 4). After sketching, the profiles are extruded at the required dimensions with the help of *Pad* modelling tool (available in *Sketch Based Features* toolbar), hereby two solids being generated.

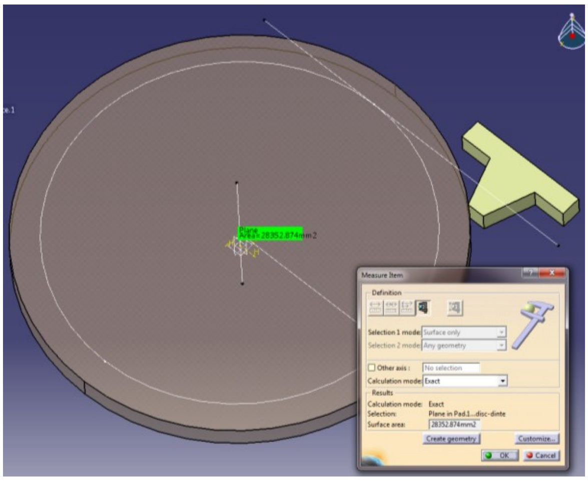

Fig. 4. Workpiece and tool tooth sketching & positioning

- Motions according to generating process specific kinematics are imposed to both solids from above. The motions are supposed to be discrete, having $\Delta\varphi$ and $\Delta\lambda$ increments, where $\Delta\varphi$ is the increment in workpiece rotation motion, corresponding to $\Delta\lambda$ increment in tool rectilinear motion. The two increment obey to the rolling condition:

$$\Delta\lambda = R_r \cdot \Delta\varphi \,. \tag{18}$$

The value of $\Delta\varphi$ during the generating process may vary after a given law.

- The shape of the effectively generated tooth flank results after representing and intersecting the successive positions of tool cutting edge.
- The theoretical involute profile is determined through the coordinates of a large enough number of points belonging to it, calculated in MatLab by using involute parametric equations.
- The list formed by these coordinates is imported in CATIA, and a spline curve is generated, by joining the corresponding points. This curve means the tooth flank theoretical profile.
- The theoretical and the effectively generated profiles are overlapped in *Part* module from CATIA, by making the symmetry axis of the two profiles to be coincident. After that, the distance between profiles is measured with *Measure between* tool, set to find the maximum distance between profiles, the measuring point automatically moving itself in the position corresponding to local maximum deviation for each position of tool cutting edge. In this way, the geometrical roughness is revealed.

## 4. NUMERICAL APPLICATION

The geometrical roughness has been assessed in an actual case of machining process, more specific, when toothing a gear with z = 60 teeth and having the module m = 10 mm. Both approaches from above were successively applied.

The analytical approach has been implemented through a dedicated MatLab application.

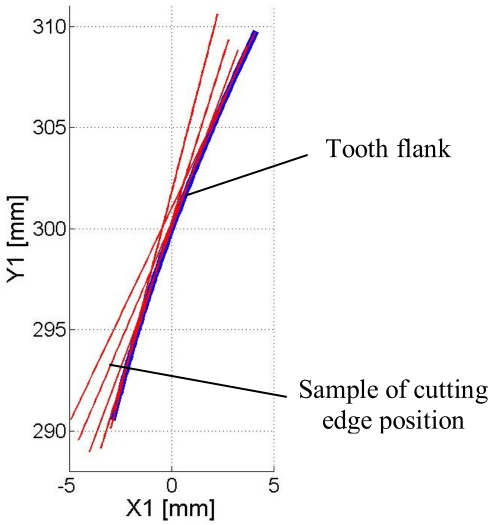


Fig. 5. Profile of the generated tooth flank

In Fig. 5 one can see the tooth involute profile (drawn with thicker line), resulted by joining $n_u = 100$ points whose coordinates were calculated with equations (12). Some successive positions of the tool cutting edge, obtained by giving sample values to φ angular parameter in (6), are also depicted, with thinner lines.

The coordinates of $N_i$ point, where the lines $\Delta_i$ and $\Delta_{i+1}$, meaning two successive cuts of the tool tooth do intersect (Fig. 3), have been found by numerically solving the system formed by (13) and (14), [9]. Both lines have been meshed in $n$ = 20,000 points and the distance between $j^{th}$ point from $\Delta_i$ and $k^{th}$ point from $\Delta_{i+1}$ is calculated with

$$d_{jk} = \sqrt{\left(X_j - X_k\right)^2 + \left(Y_j - Y_k\right)^2},\ \ j,k = 1..n. \qquad (19)$$

When $d_{jk} \le 10^{-3}$, $N_i$ coordinates are adopted as $(X_j, Y_j)$. After that, the application searches for the point from the theoretical profile which is closest to $N_i$, and the corresponding distance is considered the local value of the geometric roughness, $\lambda_i$.

According to feed variation law that enables to obtain a quasi-constant area of detached chip (Fig. 1), the highest feed values (hence the highest risks of too high geometrical roughness) are at foot and ? at head of the generated tooth. For this reason, we have simulated the tooth generating process as performed entirely with the maximum value of the circular feed, corresponding to $\varphi_{i+1} - \varphi_i = 0.01$ rad. We have run three times the application, for $\varphi_1$ = -0.105 rad, $\varphi_2$ = -0.005 rad and $\varphi_3$ = 0.095 rad, in order to find local values of the geometrical roughness at tooth foot, middle and head, respectively. The results are:

- $N_1$(-307.8855, 3.2147) and $\lambda_1$ = 0.016 mm
- $N_2$(-301.4941, 0.5509) and $\lambda_2$ = 0.039 mm
- $N_3$(-291.9338, -2.5351) and $\lambda_3$ = 0.028 mm

The graphical approach has been applied as explained above, in the same toothing case and for the same hypothesis concerning the circular feed value.

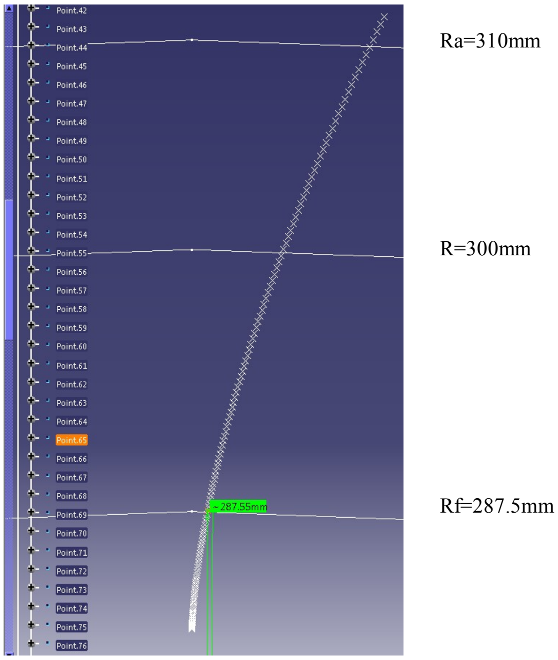


Fig. 6. Involute theoretical profile

The coordinates of the points from theoretical involute profile, calculated in MatLab, have been imported in CATIA and joined by a spline curve (see Fig. 6).

In Fig. 7 are presented the successive cuts of the tool tooth, simulated in CATIA. By intersecting the successive positions of tool cutting edge, the coordinates of $N_i$ points (Fig. 3) result and thus the geometrical roughness can be measured. In the addressed numerical application, the geometrical roughness values are presented in Fig. 8.

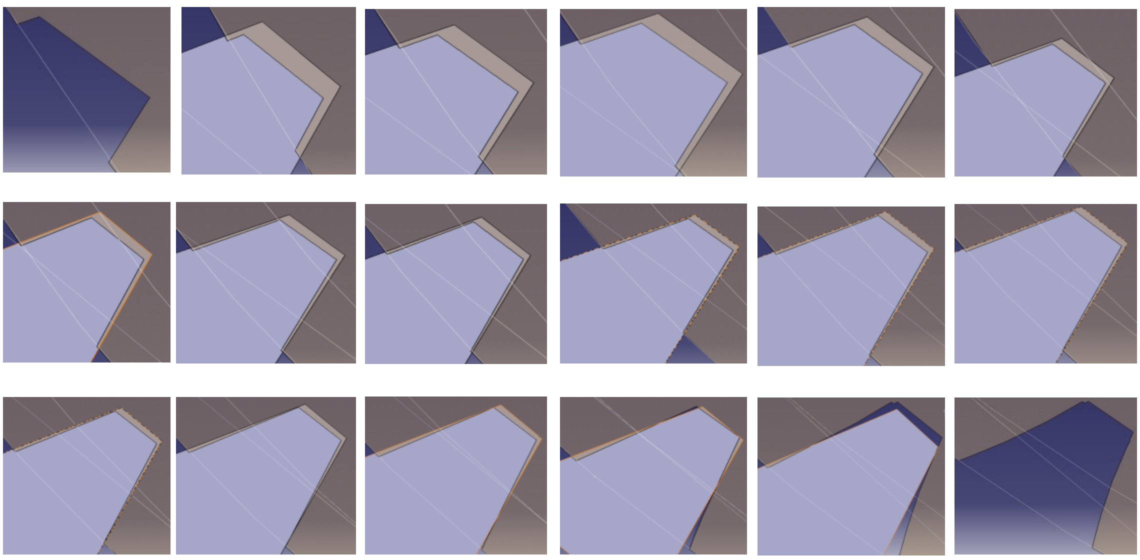

Fig. 7. Successive cuts of tool tooth

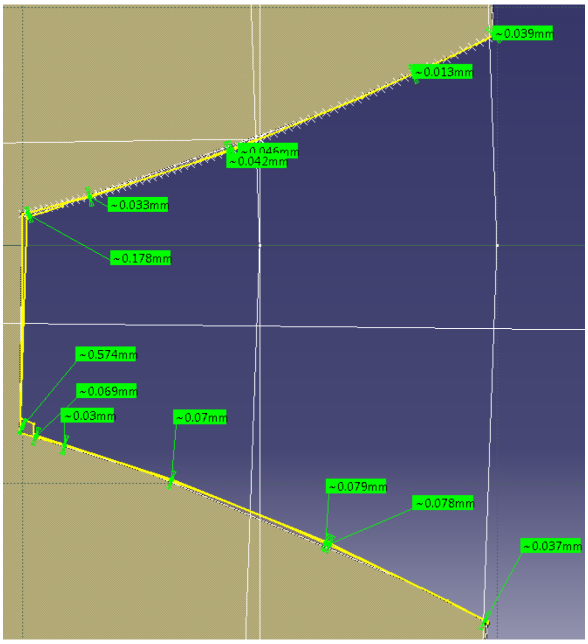


Fig. 8. Geometrical roughness graphically assessed

By comparing the results obtained by successively applying the two approaches in the same case, we should notice, above all, that they are of the same range, which is completely acceptable if we have in view the generated tooth dimension. The differences appear because the measurements were not made in exactly the same points, but also due to the errors induced by numerically solving the system formed by (13) and (14).

## 5. CONCLUSION

In this paper, two different approaches (analytical and graphical) have been considered in order to assess the geometrical roughness occurring when machining the gear tooth having involute profile, with speed motion of variable speed. Algorithms for their application have been developed and implemented in MatLab and CATIA, respectively. The numerical results obtained by performing a numerical simulation, in an actual case, show, beyond both solutions functionality, the feasibility of gears toothing with speed motion of variable speed aiming to uniform the detached chip area, at least in what concerns geometrical roughness of the generated surfaces.

## REFERENCES

[1] **Vakondios, D., Kyratsis, P., Yaldiz, S., Antoniadis, A.**, *Influence of milling strategy on the surface roughness in ball end millingof the aluminum alloy Al7075-T6*, Measurement, Vol. 45, 2012, pag. 1480-1488;

[2] **Karkalos, N.E., Galanis, N.I., Markopoulos A.P.**, *Surface roughness prediction for the milling of Ti–6Al–4V ELI alloy with the use of statistical and soft computing techniques*, Measurement, Vol. 90, 2016, pag. 25-35;

[3] **Munoz-Escalona, P., Maropoulos**, **P.G.**, *A geometrical model for surface roughness prediction when facemilling Al 7075-T7351 with square insert tools*, Journal of Manufacturing Systems, Vol. 36, 2015, pag. 216-223;

[4] **Li, Z. & Liu, Q.**, *Surface topography and roughness in hole-making by helical milling*, Int J Adv Manuf Technol, Vol. 66, 2016, pag. 1415–1425;

[5] **Damianakis, M.A., Bement, M.T., Liang, S.Y.**, *Kinematics prediction and experimental validationof machined surface roughness*, Int J Adv Manuf Technol, Vol. 65, 2013, pag. 1651–1657;

[6] **Dima, M., Oancea, N.**, *Constructive modification for the energetically improvement of the toothing process*, Romanian Journal of Technical Sciences, Applied Sciences, Vol. 49, 2004, pag.237-241.

[7] **Bordeanu, M., Frumuşanu, G., Oancea, N.,** *The energetic load smoothing along the rack tool cutting edge in toothing process*, MATEC Web of Conferences, 112, 01008, 2017.

[8] **Oancea, N.**, *Surfaces generation through winding, vol. I – III,* Galati University Press, Galați, 2004;

[9] **Frumuşanu**, **G.**, *Metode numerice în ingineria tehnologică*, Cartea universitară, Bucureşti, 2004.